AD-A125 124 ANNUAL REPORT NUMBER 14(U) WASHINGTON UNIV SEATTLE DEPT OF ATMOSPHERIC SCIENCES 01 DEC 82 N00014-76-C-0234 1/1

UNCLASSIFIED F/G 8/12 NL

END

FILMED

DTIC

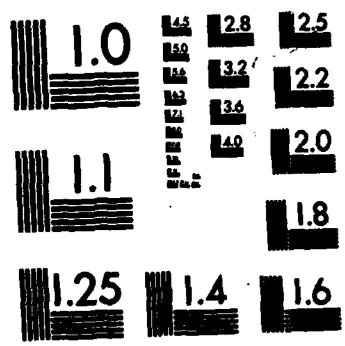

MICROCOPY RESOLUTION TEST CHART
NATIONAL BUREAU OF STANDARDS-1963-A

ANNUAL REPORT NO. 14

CONTRACT N00014-76-C-0234

NR 307-252

1 DECEMBER 1982

DEPARTMENT OF ATMOSPHERIC SCIENCES
UNIVERSITY OF WASHINGTON
SEATTLE, WASHINGTON 98195

ANNUAL REPORT NO. 14

CONTRACT N00014-76-C-0234
NR 307-252

1 DECEMBER 1982

DEPARTMENT OF ATMOSPHERIC SCIENCES
UNIVERSITY OF WASHINGTON
SEATTLE, WASHINGTON 98195

TABLE OF CONTENTS

PERSONNEL

The following scientific and technical personnel have been employed by the contract during part or all of the period covered by this report:

DR. GARY A. MAYKUT, Principal Investigator

DR. THOMAS C. GRENFELL, Research Associate

DR. DAVID A. ROTHROCK, Research Scientist

MR. RICHARD T. HALL, Mathematician

MR. DONALD K. PEROVICH, Predoctoral Associate

MS. JANE BAUER, Predoctoral Associate

INTRODUCTION

Work during this reporting period has been strongly focused on problems associated with the summer decay and retreat of the ice pack. During June and July 1982, we carried out a field program near Prince Patrick Island in the Canadian Arctic designed to clarify how solar radiation interacts with the ice and upper ocean. Measurements were taken not only in the static ice cover of Mould Bay on the south side of the island, but also in the dynamically active seasonal ice north of the island. For comparison, data gathered in the Beaufort Sea during the Arctic Ice Dynamics Joint Experiment (AIDJEX) was used to look at time dependent changes in the heat content of the upper ocean in a region of predominantly perennial ice. Both sets of results demonstrate the existence of substantial solar heating beneath the ice cover. Other calculations utilizing buoy data from the Greenland Sea support this conclusion. In fact, these results indicate that at least half of the energy involved in melting ice near the margins of the pack is supplied by the ocean. The most likely source for this energy is absorbed shortwave radiation.

Theoretical work in support of these activities has also continued. Substantial progress was made in efforts to develop a theoretical treatment of how the size distribution and number density of scattering inhomogeneities (e.g. brine pockets and vapor bubbles) in sea ice respond to changes in growth rate and ice temperature. This treatment was coupled with our radiative transfer model, allowing us to relate the optical properties of the ice to macroscopic variables such as temperature, salinity and density. A two-dimensional, time dependent diffusion model was developed for application to the problem of lateral melting in summer leads. We plan to use this model to examine the sensitivity of lateral melting to lead width and

to look at whether mechanical heat transport processes can be accounted for by suitable adjustments to the horizontal and vertical diffusivities. We are aiming at a parameterization of local melt processes suitable for inclusion in larger scale ice models. We are also working on a model which characterizes the ice cover in terms of a floe size distribution, a notion which should be of particular importance in studies of the Marginal Ice Zone (MIZ) and the summer melt cycle across the entire Arctic Ocean. The thermodynamics of the model will be based on studies such as those mentioned above. Remote sensing imagery is presently being used to investigate mechanical process (e.g. floe breakup) which will also go into the model. Results from the upcoming MIZEX in the Greenland Sea should provide invaluable data not only for understanding the thermal and mechanical forcing, but also for testing of the complete model.

SUMMER FIELD EXPERIMENT

We have just completed a month long (mid-June to mid-July) field experiment in pack ice near Prince Patrick Island in the Canadian Arctic. The base of operations was located at Mould Bay on the south side of the island. The primary objectives were: (i) to observe the salinity and temperature structure in summer leads and (ii) to infer horizontal heat transport rates from measurements of lateral melting. Observations were carried out in two main areas. A small 5-10 m lead in the motionless 2 m thick ice near Mould Bay was monitored throughout the experimental period. Measurements included vertical and lateral ablation profiles, together with salinity and temperature profiles in the lead and underlying water. Dives were made to obtain photographs of the ice edge and bottom, to take water samples from the

underside of the ice, and to perform dye experiments. The dye experiments gave a qualitative idea of water transport and mixing rates in the lead. Dye was also injected at the ice-water interface to look for the presence of boundary layer flow in the vertical. What we observed was a strong flow in the horizontal, parallel to the ice wall and the current, but no boundary layer flow. The wall profile at the ice edge was essentially vertical throughout, though some scalloping gradually developed. The ice bottom appeared smooth and uniform.

Salinity and temperature measurements were made every few days and typically consisted of vertical casts to a depth of 25 m and a series of horizontal traverses performed at four depths. In the vertical casts, measurements were taken every 10 cm for the first meter, every 20 cm from 1 to 5 m, and every meter from 5 to 25 m. At first the water in the lead was cold and salty with salinity about 32 ‰ and temperature at the salinity determined freezing point. As the melt season progressed and the lead was fed by numerous melt water streams, a fresh water layer (about 3 ‰) appeared and grew thicker, reaching the bottom of the ice by late June. By the end of the experiment the water column was characterized by three layers: (i) a warm, fresh, and well mixed upper layer (to 1.7 m), (ii) a very stable layer with a strong halocline and a temperature maximum of up to +1.5°C (1.7 to 2.7 m), and (iii) the remainder of the water column with temperature decreasing with depth and a salinity close to 32 ‰. The presence of a temperature maximum and such a strong halocline severely limited the vertical exchange of heat. Lateral ablation totaled about 0.8 m while ablation on the upper and lower surfaces totaled 1 m. The lateral ablation was due strictly to thermal processes, with no significant mechanical

erosion from waves or floe-to-floe interactions. The diurnal cycle of lead temperature was most pronounced in the upper 1.5 m, where the elevation above the freezing point ranged from .3 to .6°C over a daily cycle. Results from the horizontal traverses indicated that once the upper lead became well mixed in the vertical, it was also well mixed in the horizontal. Prior to this if gradients were evident in the vertical, they would also be present in the horizontal, although horizontal gradients were only one-tenth as great as those in the vertical.

Using records from the weather station at Mould Bay, it was possible to calculate the energy balance of the lead. Of the net energy deposited in the lead, 96% was from shortwave radiation with the remaining 4% contributed by the turbulent and longwave fluxes. Lateral melting accounted for 24% of the deposited energy, 1% warmed the water in the upper part of the lead, 35% went to bottom melting or warming of the water in the halocline above the temperature maximum, and the remaining 40% contributed to warming the water below the temperature maximum.

The other experimental area was in the dynamically active ice approximately 10 km north of the island which we were able to visit on several occasions via helicopter. Data were gathered in leads of 20, 40, 80, and 1500 m in width. In sharp contrast to the small static lead, the evidence indicated substantial amounts of lateral erosion, both mechanical and thermal. Wave cutting was evident on nearly all the floes with undercutting typically in the 2-4 m range. The amount of energy needed to produce this amount of undercutting was about 10^5 Kcal per meter of lead length. While still somewhat stratified, water in the leads appeared to be more strongly mixed than in the case of the static lead. Vertical profiles

of salinity and temperature in the 80 m wide lead, for example, revealed a 1 m thick surface layer with a salinity of 22 ^{o}/oo and temperatures ranging from -.2 to -.8°C. There was a steady increase in the amount of heat stored in the water column with time, consistent with an ice concentration of about 80%. Water temperatures ranged from 0.1 to 1.3°C above freezing. It is difficult to explain the slow rate at which the ocean apparently loses heat to the ice. We expect that observations taken during the upcoming summer MIZEX will clarify the situation.

SUMMER HEAT CONTENT OF THE UPPER OCEAN

In an attempt to learn more about the interaction of shortwave radiation with the ice and upper ocean, we have utilized oceanographic data from AIDJEX to calculate heat content in the upper 100 m of the water as a function of depth and time. Heat content (Q) was referenced to the salinity-determined freezing point of the water so that addition of low salinity melt water to the mixed layer would not affect its heat content. Changes in Q must then be due to the input of shortwave radiation or to the upward transport of warmer water from below the mixed layer.

While there were significant differences in Q(t,Z) at the four AIDJEX camps, the overall patterns were the same. Until mid-June Q was zero down to a depth of 50-60 m, below which there was a sharp gradient over a distance of 2-5 m, and then fairly constant values down to 100 m. In the latter part of June there were occasional events where the upper 50 m contained significant amounts of heat uniformly distributed in the vertical, indicating that there was still vigorous vertical mixing. Total heat content in the upper 50 m averaged about 200 cal cm^{-2} during early July,

increasing during the month to values in excess of 800 cal cm^{-2}. There was a definite maximum in Q(Z) at about 20 m, suggesting that the heating was largely due to solar radiation and that there must be a significant upward flux of heat to the ice. Despite decreases in Q in the upper 10-20 m during August, increases below this level allowed the total heat content to remain almost constant. Q began to decrease rapidly in September, giving rise to a sharp gradient in Q between 26-30 m by the end of the month. Three main layers could be distinguished throughout the fall: (i) a cold, well mixed layer (0-30 m), (ii) a layer of warmer water created during the summer (30-50 m), and (iii) deeper water whose heat content did not appear to be greatly affected by the summer melting. The thickness of the upper layer did not increase until December, after which it slowly deepened to 40-45 m by early spring.

While the mixed layer could be clearly identified from Q(Z) in the spring and fall, its extent during the summer months was less certain. In order to have an objective method of identifying the summer mixed layer, we constructed contour plots in time and depth of Brunt-Vaisala frequency (N). We found that the shallowest depth where N approached 4 cph appeared to be representative of mixed layer depth. At all camps this depth shoaled at the end of June from about 55 m to 10-15 m, after which it slowly deepened throughout the rest of the year. We then tabulated time-dependent heat content of the mixed layer, as well as that in the water below.

The results clearly indicate the presence of absorbed shortwave energy below the ice. We plan to investigate its role in more detail by utilizing other data on incident shortwave radiation, bottom ablation, and ice strain. From the strains we will first estimate chan es in ice oncentration and

then the rate of energy input to the mixed layer. Comparisons of these results with results from the heat content calculations should provide information on the amount of mixing and on the vertical transport of heat to the bottom of the ice. The consistency of these results can be checked using the data on bottom ablation.

We also noted a variety of situations whose origins were uncertain. Among these were periods at several of the camps during August where the heat content was fairly uniform from the surface down to a depth of 70-80 m. Another unexplained situation was the sudden appearance during August and September of pockets of water at the 40-60 m level with almost no heat content. Whether these are associated in some way with the eddies noted by McPhee is yet to be determined. A more careful analysis of the salinity and temperature data will hopefully shed more light on the cause of these phenomena.

Finally, we want to compare observed mass changes at the upper and lower surfaces of the ice with changes in the salt content of the upper 40-50 m of the ocean - the difference between these changes presumably being related to the amount of lateral melting on floe edges. With estimates of ice concentration and incident radiation, we should be able to get a good idea of what fraction of the solar heat input to the ocean actually goes into lateral melting. Since the STD measurements generally don't start until a depth of 4-5 m, melt water near the surface could go undetected, producing serious errors in the above calculations. However, analysis of the heat content results should tell us if the vertical mixing is sufficiently vigorous to prevent this from happening.

To help in this work, we are putting together a computer file which contains mixed layer data from each ice station (depth, heat content, salt content, etc.) and environmental parameters such as wind speed, ice velocity, and air temperature. Additional data on incident radiation, surface melting, and bottom ablation are now being processed.

SUMMER ICE DECAY MODELING

Our theoretical efforts to model heat transport and lateral melting in leads have continued with the emphasis placed on the two dimensional, time dependent diffusion model. In this model a system of equations is solved simultaneously to determine the temperature field in the lead and underlying water. The surface boundary condition is an energy balance equation depending on meteorological conditions. Radiative heating in the water is treated as a source term. Modifications were made to the model to include the presence of a boundary layer at the vertical ice-water interface and to take into account both diurnal and seasonal variations in the incident shortwave radiation.

The model has been used to conduct a series of numerical experiments investigating the effects of ice thickness, ice concentration, air temperature, cloudiness, incident radiation, and eddy diffusivities on melt rates and water temperatures in the lead. The results provide a much clearer picture of how changes in environmental forcing affect the progress of the summer melt. Increasing the air temperature from -2 to +2°C, for example, resulted in a doubling of the lateral melt rates and a roughly 70% increase in bottom melting. When the vertical and horizontal diffusivities were equal, the decrease in lateral ablation with depth was roughly exponential;

increasing the vertical diffusivity relative to that in the horizontal decreased this depth dependence. As with the simple model we used previously, the two dimensional model indicated that lateral melt rates and water temperatures are insensitive to lead width (L), once L exceeds about 100 m. This argues for the importance of knowing total floe perimeter (i.e. floe size distribution) in any attempt to model summer changes in the state and extent of the ice pack.

Field observations suggest that there are both thermal and mechanical processes involved in transporting heat from the water to the ice (and vice versa), so that a strictly thermodynamic treatment of the problem is probably inadequate. It is our hope, however, that the mechanical processes can be accounted for in the above model by suitable adjustments to the horizontal and vertical diffusivities. To test this possibility, we are presently trying to fit lateral melting profiles reported by Soviet investigators. We will also carry out similar efforts using data gathered during our recent field program in the Canadian Arctic. We expect that changes in the small static lead are due mostly to thermal processes, but that observed wall profiles in the dynamically active portion of the pack reflect the strong influence of mechanical processes. Ultimately we hope to use data from the upcoming MIZEX program to understand and quantify each of the different processes involved.

HEAT AND MASS BALANCE OF ICE IN THE GREENLAND SEA

In April 1981 J. Morison from the Polar Science Center deployed one of his ATZD buoys in the ice just north (latitude 83°N) of Greenland. The initial objective was to monitor spatial and temporal changes in the thermal

structure of the upper ocean in the Greenland Sea. Temperatures were measured by the ATZD at 10 m intervals down to a depth of 200 m. A Norwegian buoy was also deployed with the ATZD and provided data on air temperatures near the surface of the ice. During a 4 1/2 month period these buoys drifted down the Greenland Sea and through Denmark Strait where they melted out of the ice at about 68°N in mid-August. Satellite imagery indicated that this corresponded to the edge of the ice pack at that time. Substantial warming of the upper ocean took place during the last month or so of the drift, presumably the result of absorbed solar radiation and melt-water runoff. We are presently working on an analysis of these data jointly with Morison and M. McPhee in an effort to clarify the interaction of ice and upper ocean during this period.

The buoy data tell us nothing about the salinity structure of the water nor about temperatures above a depth of 20 m. We plan to infer this information using the ocean model developed by McPhee. To apply this model, we must know the heat input and density flux at the upper boundary. Techniques developed previously under this contract allow us to construct a heat and mass balance for the ice cover and to then estimate these quantities from basic data on air temperature, wind speed, cloudiness, ice concentration, and an initial knowledge of ice and snow thickness. Surface wind speeds were estimated from pressure maps of the region, ice concentration from the weekly ice charts, and cloudiness from climatology.

Although the ocean model has not been applied to the problem, thermodynamic ice model results obtained thus far demonstrate that the ocean must play an important part in the decay of the ice cover. Even with generous estimates of the incident radiation fluxes, ablation from the upper surface

totaled 50 cm of snow and 150 cm of ice. This means that more than half the ice melt had to be the result of heat supplied from the ocean. We then looked at the amount of shortwave radiation entering the ocean. With daily concentrations interpolated from the ice charts, we found that solar energy entering the water was sufficient to melt a continuous 2 m thick layer of ice, i.e. more than enough to melt all the ice not lost through surface ablation. However, some of this energy undoubtedly went into lateral melting on floe edges and was thus accounted for by the specification of ice concentration, but the exact fraction cannot yet be determined. If all the energy absorbed between the surface of the leads and the bottom of the ice went into lateral melting, then the calculations predict that the average thickness of the ice would be about 50 cm at the end of the drift; if half of this energy went to lateral melting and half to bottom ablation, the predicted thickness would be close to zero. These values are fairly sensitive to the estimated ice concentration. Increasing the ice concentration by 10%, for example, adds enough energy to the ocean to melt another 75 cm of ice during the four month period.

We conclude that the parameterizations used in the heat and mass balance model produce results consistent with what we know about the state of the ice cover, so that predictions of heat and density fluxes to the ocean should also be quite reasonable. Matching the heat input to the ocean with changes in heat content and ice mass should then allow good estimates of the density structure and vertical heat flux.

RADIATION IN SNOW AND ICE

The radiative transfer model has been modified to overcome the previous limitations imposed by refraction at the air-ice and ice-water interfaces and by approximations in the numerical representation of volume scattering. Improvements have also been incorporated to reduce computing time and to provide numerical stability for the full range of scattering and absorption of interest for sea ice and snow.

The model determines volume scattering and absorption coefficients and predicts albedos and transmissivities directly from the spatial distribution of brine pockets and vapor bubbles. To run the model at any stage, the size distribution and number density of scattering inhomogeneities must be specified. The density and radius of brine inclusions is determined from the initial brine volume and the platelet spacing, both of which can be calculated from the initial growth rate using formulae from Lofgren and Weeks (1969). The total volume of vapor in the ice is then obtained from the ice density, then for a given bubble size distribution (that of Gavrilo and Gaitshkhoki, 1970, for example) the bubble density can be determined.

During initial cooling of the ice, the temperature dependence of the brine pocket size and number density is derived from the brine volume in conjunction with a surface energy instability which causes brine channels to collapse into strings of brine pockets. The spacing of the pockets is specified by the instability mechanism and the initial diameter of the brine channels. The radius of the pockets is given by the bulk brine volume. The vapor bubble density is assumed to remain unchanged.

A subsequent warming phase is represented by the fusion of brine pockets in pairs as the brine volume increases. The brine pocket radii are assumed

to be normally distributed with a standard deviation of approximately the difference between the mean spacing and the average radius. This produces a smooth dependence of the scattering coefficient on temperature as the brine pockets enlarge, rather than the step change which would occur if every brine pocket had the same size. In addition, vapor bubbles are allowed to form in the expanding brine pockets in response to the 10% volume deficit as ice is converted to brine. This phenomenon has been observed in laboratory experiments.

To complete the representation of the warming phase, an approximation of the effect of initial brine channel formation has been included. This does not apply at temperatures near the melting point however, where brine channels completely dominate the small scale ice structure. Calculations are thus terminated when the ice temperature reaches -5°C.

The present model can now relate the optical properties of sea ice directly to readily measurable or derivable macroscopic variables such as temperature, salinity, density, and growth rate. This has enabled us to carry out parameter studies showing how the optical properties of homogeneous ice layers respond to variations in these parameters. We find, for example, that increasing the growth rate from 0.7 to 7 cm/day gives a 20% increase in the albedo at 500 nm (α_{500}) while raising the extinction coefficient (κ) by 25%. Decreasing the ice density from about 0.92 gm/cm^3 (no bubbles) to 0.86 gm/cm^3 raises α_{500} by almost 30% and κ by a factor of two.

Surprisingly, the effect of temperature variations in sea ice appears to be quite small by comparison to predictions for realistic variations in initial conditions. Contrary to our expectation that the albedo should increase with decreasing temperature, the model predicts that α_{500} is not

strongly dependent on temperature above the eutectic point - expected variations are on the order of 10%. During cooling, the effect of the increased number of brine pockets which form is balanced by the decrease in total brine volume. During warming, the formation of vapor bubbles offsets the effects of merging of the brine pockets. This suggests that the optical properties of winter and spring ice may remain fairly constant even though fairly large spatial and temporal variations in temperature are present.

When the ice temperature falls below the eutectic point however, the number density of scattering centers increases by several orders of magnitude Under these conditions α_{500} approaches unity, and the extinction coefficients rise by almost an order of magnitude.

Brine pockets appear to be the dominant scatterers because their volume density is so high, and the resulting optical depth of 1 m ice at 500 nm is on the order of 300. Since the brine pockets are strongly forward scattering due to their low contrast with pure ice, a 1 m thick layer of sea ice transmits about 10% of the net incident radiation. This is much higher than would be expected for so large an optical depth, but is quite close to what we have observed for natural sea ice. Vapor bubbles are also important, and if their effect is strong, it further masks the temperature variations.

Our calculations thus far have treated only a single homogeneous ice layer which is not realistic for most natural cases; nevertheless, the results are quite encouraging. For example, the predicted asymptotic extinction coefficients for thick ice are approximately 0.012 to 0.017 cm^{-1} in the visible, giving integrated values in excellent agreement with observations of Untersteiner (1961) and Chernigovskii (1963). Theoretical

bulk albedos, which range from about 0.6 to 0.65, are consistent with observations over pack ice. In the case of blue ice and ice below the eutectic point, a single layer approximation can be expected to apply, and in fact, agreement with observations is quite good. Spectral extinction coefficients deep within the ice, where the optical properties are expected to be homogeneous, also agree well with observed values.

Spectral albedos recently measured at Pt. Barrow are about 10% lower than the model predicts, though suggesting that enhanced levels of dust or soot may be present in the sea ice near shore. Since albedos observed in the Canadian archipelago also appear depressed when compared with Beaufort Sea results (Langleben, 1969, 1971), this may be a general effect around the margins of the Arctic Basin rather than a local phenomenon near Pt. Barrow. In the near infrared, the predicted spectral dependence of albedo does not yet agree very well with observed values. This is because the optical properties at these wavelengths depend mainly on the ice structure in the upper few millimeters where the ice is usually rather different from that found in the interior. A multilayer analysis will be needed to investigate this further.

The results of this study have been submitted for publication to the Journal of Geophysical Research. The basic model will also be applied to predictions of microwave brightness temperature. This will require some adaptation of the radiative transfer theory, but the structural aspects of the model carry over directly.

Two additional papers are currently being prepared for publication. The first involves the results of our volume scattering experiments and presents scattering functions of glacier ice and various types of laboratory

grown sea ice, including both columnar ice and grease ice. Scattering by columnar ice samples has a tensor character in that the scattering function depends on sample orientation as well as deflection angle. This effect is small though and can be ignored for the present level of observational sophistication. It was not observed for near surface and grease ice samples which have a random crystal orientation. Appropriate mean scattering functions were determined for each of the ice types studied.

Grease ice samples were found to be more highly scattering and did not have as strong a forward scattering peak as columnar ice. Glacier ice showed strong forward scattering and had a shoulder at about 80°, characteristic of vapor bubbles in ice. The forward scattering results agreed quite well with both Mie theory and ray optics calculations, but the backscattering was an order of magnitude too strong suggesting some influence of multiple scattering.

From 400 to 700 nm scattering functions are independent of wavelength. The measurements could not easily be extended to the infrared though where absorption becomes important and substantial modifications are needed in the reduction procedure.

For practical application and quantitative intercomparison, the results for sea ice were fitted to Henyey-Greenstein functions, which have a very convenient mathematical form. The data were also compared with the output of the radiative transfer model described above and found to be consistent. We have submitted this work for publication to <u>Cold Regions Science and Technology</u>.

The second paper involves our measurements of spectral albedos of sea ice and snow from 400 to 2750 nm near Pt. Barrow over the onset of the 1979

melt season. The data set, described in last year's annual report, covers the full range of ice types accessible from NARL by surface travel. Subsequent analysis suggests that it should be possible to separate out open water, snow, and melt ponds from presently available satellite imagery. Further descrimination among surface types (e.g. snow, drained first-year ice, and melting blue ice) may also be achievable, but with somewhat lower precision. This paper is presently in preparation.

FLOE SIZE DISTRIBUTION

The distribution of floe sizes affects many processes in the MIZ, among them: lateral melting, turbulent heat exchange, boundary layer drag coefficients, the resistance of ice to deformation, and the interaction of ice with surface waves. Our objective is to quantify these effects. Our first steps in this direction involve (1) developing techniques for efficiently measuring floe size distribution, (2) providing a data base for the distribution by measuring it in many regions and throughout the year, and (3) observing the details of the breakup of large floes into smaller floes, quantifying the range of piece sizes produced from the breakup of a single floe. This latter step is one process to be included in a model of the evolution of the floe size distribution as ice approaches the ice edge or as the melt season advances anywhere in the pack.

Our initial efforts have been focused on finding a simple, yet accurate, way to measure floe size distributions. Three methods were investigated using the AIDJEX summer mosaic of visual photographs, together with some LANDSAT and U-2 imagery. The first was based on finding the largest circle which could be inscribed within each floe. This proved to be too coarse

and too slow. We then tried digitizing the perimeter of every floe. This was precise and fairly quick. Finally, we sampled floe sizes using the simple technique of drawing parallel lines across an image and measuring all segments of the line lying on a floe. The distribution of these measured chords can be inverted mathematically to obtain a distribution of floe sizes. The method has the advantage of being applicable to winter pack even though distinct floes cannot be identified: then the chords are lead spacings. This method was very quick, but not as accurate as digitizing the floe perimeters. Nevertheless, measuring chords combines speed and simplicity and is probably adequate for many applications. A paper on this topic is in preparation. Included is a sampling theory which gives the variance of an estimate of floe size distribution in terms of the sample size.

In an effort to fill the void of floe size distribution observations, we have collected historical LANDSAT imagery from U.S. and European sources in the regions of the Beaufort and Greenland Seas, spanning the period 1973 to 1981. About 200 images have been selected for measurement in the Beaufort area. The years 1973 to 1976 have the better coverage in both number and spatial distribution of images. The Greenland Sea selections amount to about 100 images. Two thirds of these are from the one year 1980; the remaining images are about equally distributed in the other years. We plan to measure chord distributions in these images, then study the results for consistent patterns which may be related to seasonal or spatial variations in floe size distribution. We also plan to investigate the availability of existing aircraft data for studying floe sizes too small to be adequately resolved in the satellite imagery.

The distribution of floe sizes is controlled by divergence, lateral melting and erosion, and breakup. Each of these processes gives rise to a term in a model we are developing. The governing equation is

$$\left(\frac{\partial}{\partial t} + \underset{\sim}{u} \cdot \frac{\partial}{\partial \underset{\sim}{x}}\right) n - \frac{\partial}{\partial a} (bn) + (\text{div } \underset{\sim}{u})\ n = \mu$$

where n(a, x, t) da is the number of floes per unit area with floe area between a and a + da, $\underset{\sim}{u}$ is the horizontal ice velocity, b is the rate of change of floe area (da/dt) due to lateral melting and erosion, and μ is the rate of breakup. The important and poorly understood physics resides in the rate of size change b, and in the mechanical breakup μ. Our studies of lateral melting and the thermodynamics of leads in ablating regions, described previously, will contribute to our formulation of b, as will observations we plan to make during MIZEX 83 and MIZEX 84 on the interaction of shortwave radiation with the ice and upper ocean.

To elucidate μ, we have chosen two triplets of LANDSAT images spaced eighteen days apart, and have traced the breakup of individual floes throug each triplet. The events of breakup we have selected begin with a large floe (10-30 km diameter). At each stage the floe breaks into three to ten sizeable pieces with no more than 10% of the area broken into very small pieces. Special attention will be given to the very small fragments to determine if there is evidence of enhanced rates of decay. Using the most accurate technique, we are presently working on digitizing floe perimeters. These observations should provide some hard numbers describing breakup which will allow us to address such questions as: "How many pieces and of what sizes does a floe break into?" "Which floes break - all floes or

primarily large floes?" Future work will be directed toward determining the rate of breakup and isolating the mechanical causes. Anticipated results from MIZEX will be particularly helpful in this effort.

ICE FORMATION IN LEADS AND POLYNYAS

During January and February 1982 Jane Bauer participated in the NOAA Pacific Marine Environmental Laboratory (PMEL) overflights in the Bering and Beaufort Seas with the NOAA P-3. This aircraft, equipped with a mapping camera, SLAR, IR scanner, and gust probe, carried out both low and high level flights. Observations were made of ice growth in a polynya northwest of Barrow, Alaska, in many smaller leads in the Beaufort Sea, and at the ice edge in the Bering Sea. Photographs were obtained which document the variety of ice forms occurring in newly opened polynyas. Information obtained during these flights has been useful in determining what should be included in a two-dimensional model of ice growth in large polynyas.

Ms. Bauer has completed work on a one-dimensional numerical and laboratory model of frazil ice growth in small wind-blown leads. The model describes the situation where a strong wind blows across a lead causing wind waves and a wind-driven surface flow which then herds the frazil ice to pile up on the downwind side of the lead. As time progresses, the ice cover on the lead advances upwind and eventually covers the entire lead. Results from the numerical model show that grease ice depth increases with both wind speed and fetch. The rate of ice advance increases as the air temperature is decreased, decreases with decreasing fetch, and decreases for higher wind speeds because more ice is then required to cover the lead. Results also show that for the lowest wind speed considered (10 m s^{-1}), the grease

ice growth rates are slightly greater than the classic 'sheet' ice growth rates. However, for more extreme atmospheric conditions, the grease ice growth rates increase, becoming an order of magnitude greater than the rates for sheet ice growth at wind speeds of 30 m s^{-1}. Salt input to the ocean varies with the amount of grease ice needed to cover a given lead and the time required. The model predicts this salt flux as a function of fetch, wind speed, and air temperature. Because this ice growth mechanism allows water at its freezing point to remain in contact with the cold air, high heat and salt fluxes are maintained for substantial periods. A paper describing the model results has been accepted for publication by the Journal of Geophysical Research. The results were also presented at the December 1981 meeting of the American Geophysical Union.

We are presently working on the development of a two-dimensional model of ice growth in large polynyas. In this case frazil ice formed by wind-wave agitation of the water is herded by waves and surface flow into Langmuir streaks aligned approximately parallel to the wind. The ice in these streaks is then advected downwind by the wind waves and surface flow. As the volume of ice increases, the streaks widen and thicken. As time progresses, nilas and small pancakes with ridges on their edges form from the grease ice and are then transported downstream by both wind and wave action. As the number of floes increases, bands of these floes form which are aligned perpendicular to the wind. This model attempts to differentiate between the forcing mechanisms which cause the grease ice streaks to form parallel to the wind from those mechanisms which cause the ice floes to spread perpendicular to the wind. The model results will then be compared with available observations.

REFERENCES

Chernigovskii, N. T., Radiational properties of the ice cover of the Central Arctic, in Hydrometeorology of the Polar Regions, edited by G. Vangengeim and A. F. Laktionov, pp. 268-280, 1963. [Israel Program for Scientific Translations, ISPT 1709, 1967.]

Gavrilo, V. P. and B. Ya. Gaitskhoki, The statistics of air inclusions in ice, in The Physics of Ice, edited by V. V. Bogorodskii, pp. 125-128, 1970. [Israel Program for Scientific Translations, from Arkticheskii i Antarkticheskii Nauchno-Issledovatel'skii Institutt, Trudy, Vol. 295, Fizika l'da, 1970.]

Langleben, M. P., Albedo and degree of puddling of a melting cover of sea ice, Journal of Glaciology, 8(54), 407-412, 1969.

Langleben, M. P., Albedo of melting sea ice in the southern Beaufort Sea, Journal of Glaciology, 10(58), 101-104, 1971.

Lofgren, G.F.N. and W. F. Weeks, Effects of growth parameters on substructure spacing in NaCl ice crystals, Journal of Glaciology, 8(52), 153-164, 1969.

Untersteiner, N., On the mass and heat budget of arctic sea ice, Archiv für Meteorologie, Geophysik und Bioklimatologie, Ser. A, Bd. 12, Ht. 2, 151-182, 1961.

REPORTS PUBLISHED OR IN PROGRESS

1. Maykut, G. A., Large-scale heat exchange and ice production in the Central Arctic, Journal of Geophysical Research, 87, 7971-7985, 1982.

The arctic ice pack is a mixture of ice of many different thicknesses. Ice growth and heat exchange are strongly influenced by thickness, Particularly when the ice is thin. For this reason measurements at a particular location do not necessarily represent conditions elsewhere within the region. Large-scale heat exchange estimates must take into account contributions made by different thicknesses of ice. This requires information on the relative area covered by ice of any given thickness and on how each flux varies with thickness. Strain histories derived from the motions of several buoy and drifting station arrays were combined with climatological data on air temperatures and incoming radiation to estimate time dependent changes in the distribution of ice thickness in the Central Arctic. Thermodynamic ice models were used to determine the dependence of heat exchange and ice production on ice thickness. Large-scale fluxes were then obtained by summing the area weighted contributions made by each ice thickness category. Differences between the large-scale fluxes and those based on local measurements over perennial ice were due almost entirely to the effects of young ice less than a meter in thickness. Net annual ice production in areas of thin ice totaled about 1 m when averaged over the entire area of the strain array. In contrast to the very small annual values measured over multiyear ice, large-scale turbulent heat losses were close to 200 MJ m^{-2} $year^{-1}$, similar in magnitude to the net radiation. Absorption of shortwave radiation by summer leads resulted in annual net radiation totals for the region which were more than double those over the ice. Solar energy absorbed in the water played a major role in the mass balance of the ice cover. Intermediate thicknesses (0.2-0.8 m) of young ice, rather than open leads, exerted the greatest influence on ice production, heat input to the atmosphere, and salt input to the ocean. Monthly and annual heat flux totals obtained with different strain histories showed little correlation with the average divergence, suggesting that the variability of the strain field may be more important than the long-term average of the strain components.

2. Perovich, D. K. and T. C. Grenfell, A theoretical model of radiative transfer in young sea ice, Journal of Glaciology, 28, 341-357, 1982.

A four-stream discrete-ordinates photometric model including both anisotropic scattering and refraction at the boundaries is presented which treats the case of a floating ice slab. The effects of refraction and reflection on the redistribution of the incident radiation field as it enters the ice are examined in detail. Using one- and two-layer models, theoretical albedos and transmittances are compared to values measured in the laboratory for thin salt ice. With an experimentally determined three-parameter Henyey-Greenstein phase function, comparisons at 650 nm yield single-scattering albedos ranging from 0.95 to 0.9997. The models are then used to compare the effects of diffuse and direct-beam incident radiation, to investigate the dependence of spectral albedo and transmittance on ice thickness, and to determine the influence of very cold and melted surface layers.

3. Bauer, J. and S. Martin, A model of grease ice growth in small leads, Journal of Geophysical Research (in press).

4. Maykut, G. A., Surface heat and mass balance, in Air-Sea-Ice Interaction, Plenum Publishing Corporation, New York (in press).

5. Grenfell, T. C., A theoretical model of the optical properties of sea ice in the visible and near infrared, Journal of Geophysical Research (submitted).

6. Grenfell, T. C. and D. Hedrick, Scattering of visible and near infrared radiation by NaCl ice and glacier ice, Cold Regions Science and Technology (submitted).

7. Hanson, A. M., Observations of ice and snow in the eastern part of the Chukchi Sea - a serendipitous cruise on the Polar Sea, Arctic (submitted).

8. Grenfell, T. C. and D. K. Perovich, Spectral albedos of sea ice and incident solar irradiance in the Beaufort Sea, Journal of Geophysical Research (to be submitted).

9. Maykut, G. A. and D. K. Perovich, On the role of shortwave radiation in the decay of a sea ice cover, Journal of Glaciology (to be submitted).

10. Rothrock, D. A. and A. S. Thorndike, Floe size distributions of arctic sea ice, Journal of Geophysical Research (to be submitted).

REPORT DOCUMENTATION PAGE		READ INSTRUCTIONS BEFORE COMPLETING FORM
1. REPORT NUMBER ANNUAL REPORT NO. 14	2. GOVT ACCESSION NO. AD-A	3. RECIPIENT'S CATALOG NUMBER
4. TITLE (and Subtitle) ANNUAL REPORT NO. 14		5. TYPE OF REPORT & PERIOD COVERED INTERIM REPORT 1 OCT 1981-30 SEPT 1982
		6. PERFORMING ORG. REPORT NUMBER
7. AUTHOR(s) CONTRACT N00014-76-C-0234		8. CONTRACT OR GRANT NUMBER(s) N00014-76-C-0234
9. PERFORMING ORGANIZATION NAME AND ADDRESS ARCTIC SEA AIR INTERACTION DEPARTMENT OF ATMOSPHERIC SCIENCES AK-40 UNIVERSITY OF WASHINGTON, SEATTLE, WA 98195		10. PROGRAM ELEMENT, PROJECT, TASK AREA & WORK UNIT NUMBERS 307-252
11. CONTROLLING OFFICE NAME AND ADDRESS OFFICE OF NAVAL RESEARCH CODE 425 AR, ARCTIC PROGRAM ARLINGTON, VA 22217		12. REPORT DATE 1 DECEMBER 1982
		13. NUMBER OF PAGES 29
14. MONITORING AGENCY NAME & ADDRESS(if different from Controlling Office)		15. SECURITY CLASS. (of this report) UNCLASSIFIED
		15a. DECLASSIFICATION/DOWNGRADING SCHEDULE

16. DISTRIBUTION STATEMENT (of this Report)

THE DISTRIBUTION OF THIS REPORT IS UNLIMITED

DISTRIBUTION STATEMENT A
Approved for public release;
Distribution Unlimited

17. DISTRIBUTION STATEMENT (of the abstract entered in Block 20, if different from Report)

18. SUPPLEMENTARY NOTES

19. KEY WORDS (Continue on reverse side if necessary and identify by block number)

ARCTIC OCEAN
- Heat Exchange
- Sea Ice

SEA ICE
- Arctic Ocean
- Bering Sea
- Growth
- Heat Balance
- Lateral Melting
- Marginal Ice Zone
- Optical Properties

20. ABSTRACT (Continue on reverse side if necessary and identify by block number)

This report summarizes research performed under Contract N00014-76-C-0234, NR 307-252, during the year 1 October 1981-30 September 1982. The project is focused on problems related to the summer decay and retreat of a sea ice cover. Research topics include: (i) interaction of shortwave radiation with the ice and upper ocean, (ii) lateral melting and erosion in leads, (iii) floe size distribution, (iv) optical properties of ice and snow, and (v) ice growth in large leads and polynyas. Field work was carried out near Prince Patrick Island in the Canadian Arctic and over the ice pack in the Bering Sea.

DD FORM 1 JAN 73 1473 EDITION OF 1 NOV 65 IS OBSOLETE
S/N 0102-014-6601

DISTRIBUTION LIST

CONTRACT N00014-76-C-0234
NR 307-252

DEFENSE TECH INFO CENTER
CAMERON STATION
ALEXANDRIA, VA 22314

US NAVAL RESEARCH LABORATORY
CODE 2627
WASHINGTON, DC 20375

WOODS HOLE OCEANOGRAPHIC INST
DOCUMENT LIBRARY LO-206
WOODS HOLE, MA 02543

COLD REGIONS RES & ENG LAB
72 LYME ROAD
HANOVER, NH 03755

DR JOHN C F TEDROW
SOILS & CROPS DEPT, COOK COLLEGE
RUTGERS UNIVERSITY, PO BOX 231
NEW BRUNSWICK, NJ 08903

DEPARTMENT OF THE ARMY
OFFICE CHIEF OF ENGINEERS
ATTN DAEN-RDM (DR GOMEZ)
WASHINGTON, DC 20314

POLAR RESEARCH BOARD
NATL ACADEMY OF SCIENCES
2101 CONSTITUTION AVENUE, NW
WASHINGTON, DC 20418

POLAR INFORMATION SERVICE
OFFICE OF POLAR PROGRAMS
NATIONAL SCIENCE FOUNDATION
WASHINGTON, DC 20550

DR FRANCIS S L WILLIAMSON
CHIEF SCIENTIST
OFFICE OF POLAR PROGRAMS, RM 620
NATIONAL SCIENCE FOUNDATION
WASHINGTON, DC 20550

MR M M KLEINERMAN
PROJECT MANAGER FOR ARCTIC ASW
US NAVAL SURFACE WEAPONS CENTER
WHITE OAK, SILVER SPRING, MD 20910

DR G LEONARD JOHNSON
CODE 425 ARCTIC
OFFICE OF NAVAL RESEARCH
ARLINGTON, VA 22217

CHIEF OF NAVAL RESEARCH
OFFICE OF NAVAL RESEARCH
CODE 425 ARCTIC
ARLINGTON, VA 22217

NAVAL FACILITIES ENG COMMAND
CODE 04B
200 STOVALL STREET
ALEXANDRIA, VA 22332

US NAVAL OCEANOGRAPHIC OFFICE
LIBRARY (CODE 8160)
NSTL STATION
BAY ST LOUIS, MS 39522

DIRECTOR, INST OF POLAR STUDIES
OHIO STATE UNIVERSITY
125 SOUTH OVAL MALL
COLUMBUS, OH 43210

DR ALBERT H JACKMAN
CHAIRMAN, DEPT OF GEOGRAPHY
WESTERN MICHIGAN UNIVERSITY
KALAMAZOO, MI 49008

DR PHILIP P MICKLIN
DEPARTMENT OF GEOGRAPHY
WESTERN MICHIGAN UNIVERSITY
KALAMAZOO, MI 49008

DR REID A BRYSON
INST FOR ENVIRONMENTAL STUDIES
UNIVERSITY OF WISCONSIN
MADISON, WI 53706

DR DAVID CLARK
DEPARTMENT OF GEOLOGY
UNIVERSITY OF WISCONSIN
MADISON, WI 53706

DISTRIBUTION LIST, CONTRACT N00014-76-C-0234, NR 307-252

DR HARLEY J. WALKER
DEPARTMENT OF GEOGRAPHY
LOUISIANA STATE UNIVERSITY
BATON ROUGE, LA 70803

MR TERRY RALSTON
EXXON RESEARCH PRODUCTION CO
PO BOX 2189
HOUSTON, TX 77001

WORLD DATA CENTER: A FOR GLAC
CIRES, CAMPUS BOX 449
UNIVERSITY OF COLORADO
BOULDER, CO 80309

LIBRARY (CODE L08A)
NAVAL CIVIL ENGINEERING LAB
PORT HUENEME, CA 93043

T JOSEPH HOLLAND
CODE L51
NAVAL CIVIL ENGINEERING LAB
PORT HUENEME, CA 93043

MR BEAUMONT BUCK
POLAR RESEARCH LAB INC
123 SANTA BARBARA STREET
SANTA BARBARA, CA 93101

DR W M SACKINGER
GEOPHYSICAL INSTITUTE
UNIVERSITY OF ALASKA
903 KOKUYUK AVENUE NORTH
FAIRBANKS, AK 99701

DR KEITH MATHER
705 GRUENING BUILDING
UNIVERSITY OF ALASKA
FAIRBANKS, AK 99701

PROF J L BURDICK
CIVIL ENGINEERING DEPT
UNIVERSITY OF ALASKA
306 TANANA DRIVE
FAIRBANKS, AK 99701

DR GUNTER WELLER
GEOPHYSICAL INSTITUTE
UNIVERSITY OF ALASKA
FAIRBANKS, AK 99701

INUVIK SCIENTIFIC RESOURCE CENTRE
DEPT INDIAN AND NORTHERN AFFAIRS
BOX 1430
INUVIK, NW TERRITORIES X0E 0T0
CANADA

DR SVENN ORVIG
MCGILL UNIVERSITY
DEPT OF METEOROLOGY
805 SHERBROOKE STREET WEST
MONTREAL, PQ H3A 2K6 CANADA

OCEANOGRAPHY LIBRARY
MCGILL UNIVERSITY
3620 UNIVERSITY STREET
MONTREAL, PQ H3A 2B2 CANADA

DR E R POUNDER
RUTHERFORD PHYSICS BLDG
MCGILL UNIVERSITY
3600 UNIVERSITY STREET
MONTREAL, PQ H3A 2T8 CANADA

METEOROLOGY LIBRARY
MCGILL UNIVERSITY
805 SHERBROOKE STREET WEST
MONTREAL, PQ H3A 2K6 CANADA

NORTHERN STUDIES LIBRARY
MCGILL UNIVERSITY
1020 PINE AVENUE WEST
MONTREAL, PQ H3A 1A2 CANADA

DEPARTMENTAL LIBRARY-SERIALS
DEPT OF THE ENVIRONMENT
OTTAWA, ONTARIO K1A 0H3 CANADA

DR E L LEWIS
FROZEN SEA RESEARCH GROUP
INSTITUTE OF OCEAN SCIENCES
9860 W SAANICH ROAD, PO BOX 6000
SIDNEY, BC V8L 4B2 CANADA

LIBRARIAN
DEFENCE RES ESTABLISHMENT PAC
FORCES MAIL OFFICE
VICTORIA, BC V0S 1B0 CANADA

METEOROLOGICAL OFFICE LIBRARY
LONDON ROAD
BRACKNELL, BERKSHIRE, ENGLAND

DISTRIBUTION LIST, CONTRACT N00014-76-C-0234, NR 307-252

SEA ICE GROUP
SCOTT POLAR RESEARCH INSTITUTE
CAMBRIDGE, CB2 1ER ENGLAND

THE LIBRARIAN
SCOTT POLAR RESEARCH INSTITUTE
CAMBRIDGE, CB2 1ER ENGLAND

DR MICHAEL KELLY
SCHOOL OF ENVIRONMENTAL SCIENCES
UNIVERSITY OF EAST ANGLIA
NORWICH, NR4 7TJ ENGLAND

LIBRARIAN
INST OF OCEANOGRAPHIC SCIENCES
WORMLEY, GODALMING, SURREY
GU8 5UB UNITED KINGDOM

CENTRE NATL DE LA RECHERCHE SCI
LABORATOIRE DE GLACIOLOGIE
UNIVERSITE DE GRENOBLE 1
SERV DE GEOPHYS, 2, RUE TRES
CLOITRES 38-GRENOBLE, FRANCE

CENTRE D'ETUDES ARCTIQUES
19 RUE AMÉLIE
75007 PARIS, FRANCE

DR KOU KUSUNOKI
NATL INST OF POLAR RESEARCH
9-10, KAGA 1-CHOME
ITABASHI-KU, TOKYO 173
JAPAN

DR TORGNY VINJE
NORSK POLARINSTITUTT
ROLFSTANGVN 12, POSTBOKS 158
1330 OSLO LUFTHAVN
NORWAY

DR KNUT AAGAARD
DEPARTMENT OF OCEANOGRAPHY WB-10
UNIVERSITY OF WASHINGTON
SEATTLE, WA 98195

DR LAWRENCE COACHMAN
DEPARTMENT OF OCEANOGRAPHY WB-10
UNIVERSITY OF WASHINGTON
SEATTLE, WA 98195

DR SEELYE MARTIN
DEPARTMENT OF OCEANOGRAPHY WB-10
UNIVERSITY OF WASHINGTON
SEATTLE, WA 98195

UNIVERSITY ARCHIVES
UNIVERSITY RECORDS SECTION BL-10
UNIVERSITY OF WASHINGTON
SEATTLE, WA 98195

DR NORBERT UNTERSTEINER
APPLIED PHYSICS LABORATORY HN-10
UNIVERSITY OF WASHINGTON
SEATTLE, WA 98195

MR L JON BUTTARS
OFFICE OF NAVAL RESEARCH JD-27
UNIVERSITY OF WASHINGTON
SEATTLE, WA 98195